J. Med. Biol. Eng. (2017) 37:288–297
DOI 10.1007/s40846-017-0223-7

ORIGINAL ARTICLE

A Modeling Study on Inspired CO_2 Rebreathing Device for Sleep Apnea Treatment by Means of CFD Analysis and Experiment

Mehdi Shokoueinejad[1,4] · Arman Pazouki[2] · Jake Levin[1] · Fa Wang[3] · Chris Fernandez[1] · Samuel Rusk[3] · Ícaro dos Santos[1] · Ashley Mulchrone[1] · Jerome Dempsey[4] · John G. Webster[1]

Received: 25 July 2016 / Accepted: 3 January 2017 / Published online: 27 March 2017

Abstract We present the device design, simulation, and measurement results of a therapy device that potentially prevents sleep apnea by slightly increasing inspired CO_2 through added dead space (DS). The rationale for treatment of sleep apnea with CO_2 manipulation is based on two recently reported premises: (i) preventing transient reductions in $PaCO_2$ will prevent the patient from reaching their apneic threshold, thereby preventing "central" apnea and instabilities in respiratory motor output; and (ii) raising $PaCO_2$ and end-tidal CO_2, even by a minimal amount, provides a strong recruitment of upper airway dilator muscles, thereby preventing airway obstruction. We have also provided the simulation results, obtained from solving the Navier–Stokes (NS) equations within the device volume. Therein, the NS equations are coupled with a convection–diffusion equation that represents the transport of CO_2 in the device, thus enabling the transient simulation of CO_2 propagation. Using this procedure, a prototype of variable volume dead space reservoir device was designed. Volumetric factors influencing carbon dioxide increases in the added reservoir (open-ended DS) were investigated. The maximum/minimum amount of CO_2 concentration were obtained for the maximum/minimum device volume; 3.4 and 2.4 mol/m^3 for the DS volumes of 1.2 and 0.5×10^{-3} m^3, respectively. In all case studies, the CO_2 buildup reached a plateau after approximately 20 breathing cycles. The experimental measurement results are in agreement with the simulation and numerical results obtained using the proposed simplified modeling technique, with a maximum relative error of 3.5%.

Keywords Sleep apnea · Inspired carbon dioxide CO_2 · Computational fluid dynamics · Transport of diluted species

Abbreviation

P_aCO_2	Atrial Pressure of Carbon Dioxide in Arterial Blood
$P_{ET}CO_2$	End tidal CO_2
x_{O_2}	Concentration of O_2
x_{CO_2}	Concentration of CO_2
$x_{O_2,1}$	Chamber O_2 concentration before inhale
$x_{O_2,2}$	Chamber O_2 concentration after inhale
$x_{O_2,3}$	Chamber O_2 concentration after exhale
$x_{O_2,in}$	Inlet air O_2 concentration
$x_{CO_2,2}$	Average CO_2 concentration after inhale
$y_{O_2,1}$	Average inhale air O_2 concentration
$y_{O_2,2}$	Average exhale air O_2 concentration
$c_{n,1}^{ave}$	Average CO_2 concentration after inhale where n is the breathing cycle number
$c_{n,2}^{ave}$	Average CO_2 concentration after exhale in nth breathing cycle
v_b	Air velocity at the inlet boundary
TV	Tidal Volume
RV	Reservoir Volume

✉ Mehdi Shokoueinejad
mehdi@bme.wisc.edu

[1] Department of Biomedical Engineering, University of Wisconsin-Madison, Madison, WI 53706-1572, USA

[2] Department of Mechanical Engineering, California State University, Los Angeles, CA 90032, USA

[3] Department of Electrical Engineering, University of Wisconsin-Madison, Madison, WI 53706-1572, USA

[4] The John Rankin Laboratory of Pulmonary Medicine, Medical Sciences Center, University of Wisconsin-Madison, Madison, WI 53706-1572, USA

γ Main reason to introduce γ in the equations is to (i) account for imperfect mixing in small volume, e.g. due to undeveloped flow and (ii) account for any unforeseen parameter that can affect the mixing of CO_2 and fresh air

1 Introduction

An escalating 10% of the general US population has clinically significant sleep apnea [1], where breathing stops repeatedly and interrupts sleep, leading to significant cardio-vascular morbidities, insulin resistance, neural injury, heart attack, irregular heartbeat, and accelerated mortality. These effects of sleep apnea lead to a decrease in quality of life and productivity. Sleep apnea may increase the risk for accidents while working or driving.

One possible treatment for sleep apnea is the use of inspired CO_2. Since the early 1980s, several studies have shown that the constant inhalation of CO_2 can help prevent central sleep apneas (CSA) [2–7]. Even obstructive sleep apnea (OSA) patients with extremely collapsible airways responded positively to the CO_2 treatment Most of these results were obtained during periods of 1 to 6 h of CO_2 therapy during the night [8].

Although upper airway collapsibility is a critical component of OSA, it is now well-established that pathophysiologic characteristics such as a sensitive arousal threshold (to elicit ventilatory overshoots), high "loop gain" i.e. chemo-sensitivity and plant gain, and/or reduced responsiveness of airway dilator musculature to chemoreceptor stimulation are also commonly present in the majority of OSA patients [9, 10]. In turn, CO_2 has been shown to be a major regulator of airway caliber during sleep, i.e. when the "wakefulness" stimulus is removed, as evidenced by the following observations: (1) small transient reductions in P_aCO_2–as experienced with ventilatory overshoots which occur upon recovery from an apnea and/or via transient arousals—of 1–4 mmHg will elicit apneas and ventilatory instability during NREM sleep [11, 12]; (2) adding inspired CO2 sufficient to increase P_aCO_2 1–3 mmHg removes most or all of the hypocapnic induced central apneas and the periodic breathing induced via hypoxic exposure and/or CHF, spinal cord injury, or with idiopathic central apnea [13–17]; and (3) adding inspired CO_2 increases both phrenic (linear) and hypoglossal (alinear) motor nerve activity, thereby recruiting both diaphragm and upper airway dilator muscles [18, 19].

So theoretically, increasing CO_2 should stabilize central respiratory motor output as well as improve upper airway caliber and prevent upper airway obstruction. It is believed that breathing in low concentrations of CO_2 can help prevent periodic reductions in P_aCO_2. By preventing these levels from falling below the apnea threshold of P_aCO_2, the number of breathing cessations can be reduced. However, handling all the equipment for exogenous CO_2 can be cumbersome in a household setting, and the benefits towards sleep quality are still debated [6, 20, 21]. Another method of increasing CO_2, is the addition of extra DS. Dead space is the portion of the airway passages that do not contribute to gas exchange (i.e. trachea and bronchi). It has been shown that the Apnea-Hypopnea Index (AHI) in CSA and OSA patients can be decreased by the addition of as little as 400 to 600 mL of external DS [8, 22, 23]. A study showed that 17 of 21 OSA patients subjected to mild to moderate levels of rebreathing their own CO_2 during sleep eliminated most of their sleep disordered breathing [8]. This study used a "fixed" volume rebreathing device worn using a full face mask.

These findings by using DS raised the question of how rebreathing of exhaled gas affects subsequent CO_2 accumulation/concentration rate change. In addition to the experimental study of such problems, computer simulation provides an alternative way of validating the DS-based experiment by considering a range of parameters that affect the CO_2 concentration, thus allowing for the analysis of a larger group of subjects. Unfortunately, the literature is void of any computational modeling. At the very best, a mathematical modeling of the CO_2 accumulation in *closed* spaces is provided in [24]. This model; however, is not extendable to the current study since the apnea treatment device considered herein is an open end volume.

The present study aims to investigate the effects of DS volume on CO_2 concentrations through simulation and experimentation. The aim is to propose, quantify, and validate the CO_2 accumulation in the proposed device designs. The remainder of the document is organized as follows. Section 2 elaborates on the design of the device that is used to treat the sleep apnea. A computational approach is explained and adopted in Sect. 3.1. The simulation and experiment results for various device volumes are provided in Sect. 3.2. A mathematical model to capture the CO_2 accumulation in the open-volume apnea treatment device is discussed in Sect. 3.3. Section 4 provides further discussion of the results.

2 Device Design

A variable volume DS reservoir device was designed for the purpose of validating the mathematical model formulated in this study [25]. The design of our device incorporated an automatic variable DS volume, different from previous models which involved the fixed volume. Our device's main criterion was to allow for incremental adjustments in length to vary the DS present in the device.

The varied DS volume's objective is to create different CO_2 concentrations inside the device's reservoir for rebreathing. The CO_2 concentration is measured at different volume intervals to determine the effect of DS volumes on CO_2 concentrations.

A generic embodiment of the device consists of a mask to cover the wearer's mouth and nose, the mask is connected via a flexible tube to a variable sized reservoir that has an inlet, connected to the tube, and an outlet which is open for fresh air ventilation. The distance between inlet and outlet is adjustable. The main feature of this device is the variably sized reservoir. Different physical devices can be constructed to create this variably sized reservoir that has an adjustable length between the inlet and outlet. One such embodiment of the reservoir consists of a worm-gear driven bellow tube to position its base which allows the contraction and expansion of a constant diameter cylinder to a desired volume.

The embodiment's external housing and threaded disc, pictured in Fig. 1, were fabricated using 3D printing. The motor was mounted to the left side of the housing using screws. The worm gear was attached to the motor via a hole on the left wall. The threaded disc that acts as the outlet for the DS was then screwed halfway down the shaft. A plastic bellow was stretched over the threaded disc and secured to a lip at the left wall of the device that encompasses the inlet hole. With the internal components assembled, a top to the housing was screwed on the right side of the device, closing the reservoir and centering the worm gear with a ball bearing in the top. An Arduino processor was then mounted in an electronics box and screwed to the housing to process the sensors and control the motor.

The device controls the CO_2 concentrations by moving the threaded disc and changing the DS volume. By varying the volume of the DS, exhaled CO_2 builds up in the DS and does not get recycled into the ambient surroundings. The exhaled CO_2 mixes with ambient air in the DS to raise the CO_2 concentrations in the rebreathed DS. Once the user inhales, the excess CO_2 from the DS raises the CO_2 concentration in the user. CO_2 levels in the user are fluctuated by adjusting the amount of DS present for inhalation. The longer the DS, the more CO_2 that can accumulate without being ejected from the device during exhalation. When the device records a hypopnea from the patient with the device's sensors, it actuates the motor and drives the worm gear to incrementally advance the threaded disc for expansion of the DS. As more hypopneas occur, the device will keep incrementing the threaded disc until apneas discontinue. If a hyperpnoea occurs, then the device will retract the threaded disc and reduce the volume of DS the user rebreathes. This retraction will continue until no hypo-/hyperpnoea occur, at which point the device will maintain the current DS volume.

Figure 1 shows the device used for this study. Exhaled breath from the wearer comes in through the inlet on the top left side of the device and enters the DS. The DS is defined as the volume of the threaded container from the plate that connects to the open air to the plate that connects to the flexible breathing tube. The threaded disc (approximately center on Fig. 1) contains an outlet for airflow and a threaded hole that interfaces with a central worm gear (center shaft with threads in Fig. 1. A motor located below the inlet drives the worm gear that results in a translation of the threaded disc to either expand or contract the DS (an expansion would be moving the threaded disc to the right as seen in Fig. 1. The DS is contained within a larger cylindrical casing that contains square holes for the air exchange and prevents interference from external objects to the moving internal parts.

3 Analysis

3.1 Numerical Simulation

To further investigate the accumulation of the CO_2 in the rebreathing device, a numerical simulation of the transport

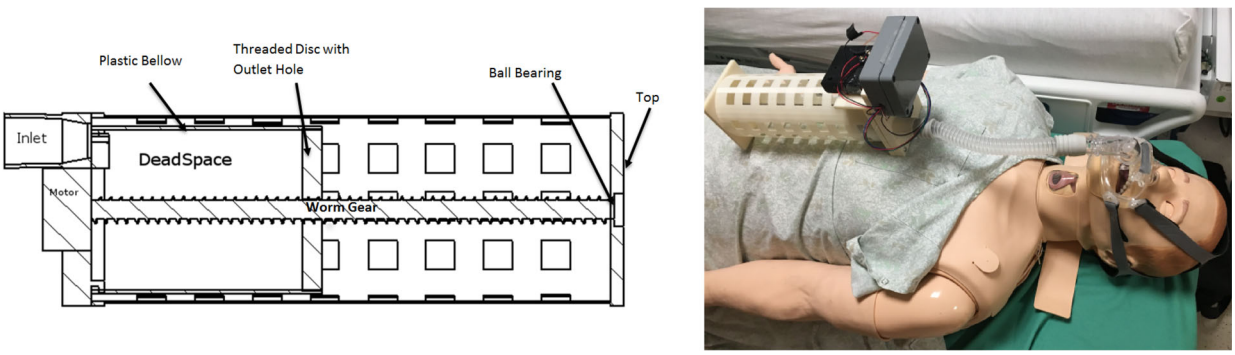

Fig. 1 *Left* Schematic diagram of an accordion-like, 8 cm diameter collapsed bellows DS. An axial stepper motor rotates a long worm gear protruding at the near end that expands the bellows up to expanded length. The larger perforated white surround (casing) prevents the patient from contacting any motion, yet permits gas flow. *Right* Mannequin using the device

of diluted species was conducted herein. The governing equation of the transient air flow in the device can be explained by Navier–Stokes (NS) and Continuity equations

$$\rho\frac{\delta u}{\delta t}+\rho(u\cdot\nabla)u=\nabla\cdot\left[-pI+\mu\left(\nabla u+(\nabla u)^T\right)\right] \quad (1)$$

$$\nabla.u=0, \quad (2)$$

where u, p, ρ and μ are the fluid velocity, pressure, density, and viscosity, respectively. The convection–diffusion of the CO_2 is expressed by [26]

$$\frac{\delta c_i}{\delta t}+\nabla.(-D_i\nabla c_i)+u.\nabla c_i=R_i, \quad (3)$$

where c_i and R_i are the CO_2 concentration and source/sink; was used to simulate ventilat$R_i=0$ in the current study due the absence of chemical reaction. D_i is the diffusivity (also called diffusion coefficient), such as mass diffusivity for particle motion. The value of diffusion coefficient D for the diffusion of CO_2 in fresh air is 0.166 cm^2/s at 310.15 T/K [27]. Equation (3) is coupled to the NS equations given in Eqs. (1) and (2).

Due to the negligible amount of CO_2 in the fresh air (<0.04%) and stationary condition before breathing, a uniform zero initial CO_2 concentration, $c_o=0$, and zero velocity were assumed in the device. The outflow boundary conditions for velocity and concentration were modeled as

$$\left[-pI+\mu\left(\nabla u+(\nabla u)^T\right)\right]n=-p_0n, \quad (4)$$

$$Dn_i\nabla c_i=0, \quad (5)$$

where p_0 is the ambient pressure.

The COMSOL software [28] was leveraged to model the CO_2 propagation explained by Eqs. (1–5). A breathing cycle was then modeled as two separate simulations to mimic the inhale and exhale processes individually. The difference of the two simulations was in the inlet concentration boundary condition as explained below:

- *Inhale* An inflow air with the CO_2 concentration $c=0$ mol/m^3, i.e. that of the fresh air, and velocity $v_b=0.35$ m/s in form of a step function was applied to the simulation [29]. At the end of the simulation, the average CO_2 concentration, $c_{n,1}^{ave}$, was measured inside the reservoir, where n is the breathing cycle number.
- *Exhale* An inflow concentration $c=20.95-(1-\frac{5}{21})c_{n,1}^{ave}$ [24] and velocity v_b was considered. The average CO_2 concentration of the reservoir, $c_{n,2}^{ave}$, was measured at the end of the process.

Zero initial velocities were considered inside the reservoir for both *Inhale* and *Exhale* cycle. The initial concentration for each cycle was the final average concentration of the previous cycle; that is, for the breathing cycle n, $c_{n,2}^{ave}$ and $c_{n,1}^{ave}$ were assigned as the initial concentration of the *Inhale* and *Exhale*, respectively.

Fluid and concentration equations, Eqs. (1–3) were solved simultaneously (fully coupled). In terms of modeling, a Reynolds-Averaged Navier–Stokes (RANS) with a $K-\epsilon$ model is used. The linear system constructed from the FEM discretization was solved using an iterative Backward Differentiation Formula (BDF-2) method at each time step until the convergence was achieved (on average around 7–9 iterations). The simulation consisted of multiple (20) breathing cycle with independent inhale and exhale simulation in each cycle (total of 40 simulations). The inlet and outlet boundary conditions were implemented using Dirichlet (for velocity and concentration) and Neumann (for pressure). The compute time to execute 40 simulations was around 18 h on a PC with an Intel I7 processor and 64 GB RAM.

In the simulation of the exhale, the inlet condition, i.e. where the exhale air entered the chamber, had a fixed velocity which was obtained from the exhale air volumetric rate in an average human (500 mL/cycle which represents the tidal volume). More specifically, we set the inlet velocity equal to 0.3 [m/s].

Similarly, the exhale concentration was fixed; the value of exhale CO_2 was calculated based on the average concentration of O_2 in inhale: $c=20.95-\left(1-\frac{5}{21}\right)c_{n,1}^{ave}$ [24] where c_{ave} is the average inhale concentration and (1–5/21) is a typical rate of O_2 consumption in one breathing cycle. The value of c_{ave} was estimated by averaging the chamber CO_2 concentration at the beginning and end of one inhale cycle. Finally, the pressure boundary condition was applied using Neumann boundary where pressure gradient was zero in the direction of the boundary. The simulation procedure for the inhale was the same as that of the exhale and the velocity and pressure boundary conditions were similar to those of the exhale. The CO_2 concentration at the inlet, i.e. where the air enters the chamber, was the same as that of the fresh air (almost zero).

As for the initial condition, we used zero velocity and atmospheric pressure in the reservoir. The value of the concentration depended on the history of the breathing through the device, i.e. the number of the simulation in the sequence of breathing cycles: at any certain simulation, we set the initial CO_2 concentration the same as that calculated from the last breathing sub-cycle (inhale or exhale).

We used variable mesh length (smaller elements at the wall, larger at the center) with a growth rate of 1.2 normal to the wall. The reason for doing this was to improve the quality of the wall boundary condition. We used the COMSOL meshing tool. Overall, the model was discretized using about 40000 Tetrahedra, Pyramid, and Prism elements, please see Fig. 9 (see Appendix). Table 1 (see

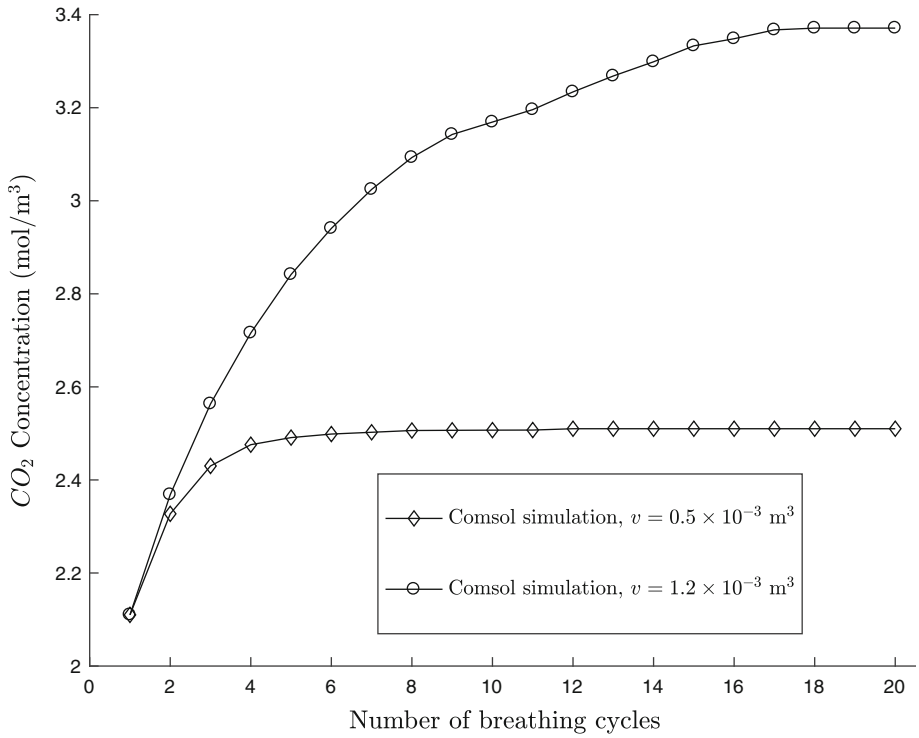

Fig. 2 Average CO_2 concentrations for device volumes v $= [0.5, 1.2] \times 10^{-3}$ m^3 obtained from simulation

Appendix) includes details about the mesh used in the computational study, such as type of elements, number of elements, and mesh quality metrics.

Two device dimensions, with DS volumes equal to v $= [0.5, 1.2] \times 10^{-3}$ m^3, were investigated. For each device n $= 20$ breathing cycles were simulated using the *Inhale* and *Exhale* procedures explained before. As shown in Fig. 2 the plateau of the average CO_2 buildup occurs before the 20th breathing cycle. Figures 3 and 4 capture the concentration development in device designs associated with the maximum and minimum volume for three time steps: t $= 0.5, 1.0, 2.4$s. A breathing cycle is assumed to take about 4.8 s, which is equivalent to 2.4 s exhale or inhale time.

3.2 Experimental Study Model

A pediatric human patient simulator (HPS) mannequin, Fig. 1, *right,* was used to simulate ventilation to measure the CO_2 accumulation in a reservoir for two volumes of v $= 0.5 \,\&\, 1.2 \times 10^{-3}$ m^3. The mannequin 'breathed' with tidal volume 500 mL and expired CO_2 concentration of 5% $= 2.11$ (mol/m^3). End-tidal CO_2 ($P_{\mathrm{ET}}CO_2$) and level of CO_2 were recorded using a CARDIOGRAPH® by Respironics monitoring system.

3.3 Mathematical Modeling

To further simplify the numerical studies, a mathematical model may be used to evaluate the accumulation of CO_2. A similar effort was made in [24] to evaluate the accumulation of CO_2 due to rebreathing in a confined space. Therein, the CO_2 accumulation was formulated as

$$x_{O_2,2} = \left[(RV - TV)x_{O_2,1} + TV\left(1 - \frac{5}{21}\right)x_{O_2,1}\right] \Big/ RV \tag{6}$$

$$x_{CO_2,2} = \left[8.83\,\frac{\mathrm{mol}}{\mathrm{m}^3} - x_{O_2,2}\right], \tag{7}$$

where x_{O_2} and x_{CO_2} are the concentration of O_2 and CO_2 in mol/m^3, respectively; TV is the tidal volume which is assumed to be 4.5×10^{-4} m^3; and RV is the reservoir volume in which the rebreathing occurs. Equations (6) and (7) predict a continues increase in the CO_2 to its maximal value, i.e. 8.83 mol/m^3. Our proposed device is an open-space reservoir with a hole to allow for outflow of expired air and inflow of fresh air. Therefore, Eqs. (6) and (7) are not suitable for the current study. A model is proposed herein to describe the CO_2 accumulation inside an open-space reservoir. By allowing a reservoir connection to the

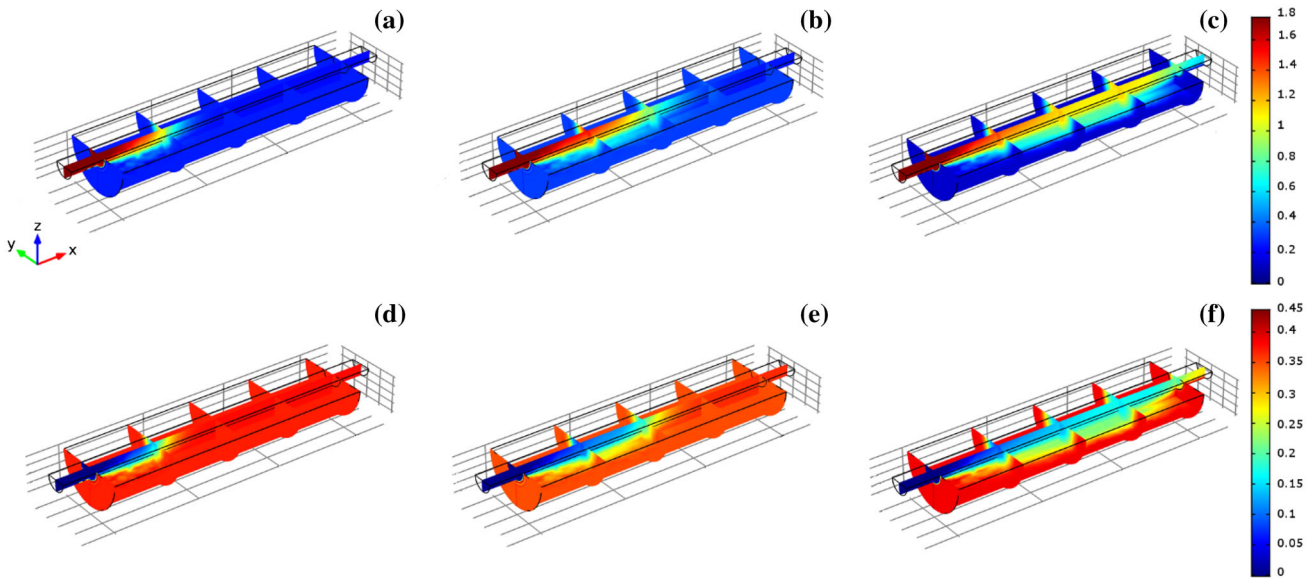

Fig. 3 Transient CO_2 concentration (mol/m^3) propagation in a reservoir with the volume v $= 1.2 \times 10^{-3}$ m^3 at three time instances: t = 0.5s (**a**, **d**), t = 1.0s (**b**, **e**), t = 2.4s (**c**, **f**). **a**–**c** and **d**–**f** denote the exhale and inhale processes, respectively. The inflow boundary condition is assumed at the *left* side of the reservoir. In **a**–**c** the *left side* denotes the *inlet* of accordion-like device, and in **d**–**f**, *left* side denotes the outlet of accordion-like device presented in Fig. 1

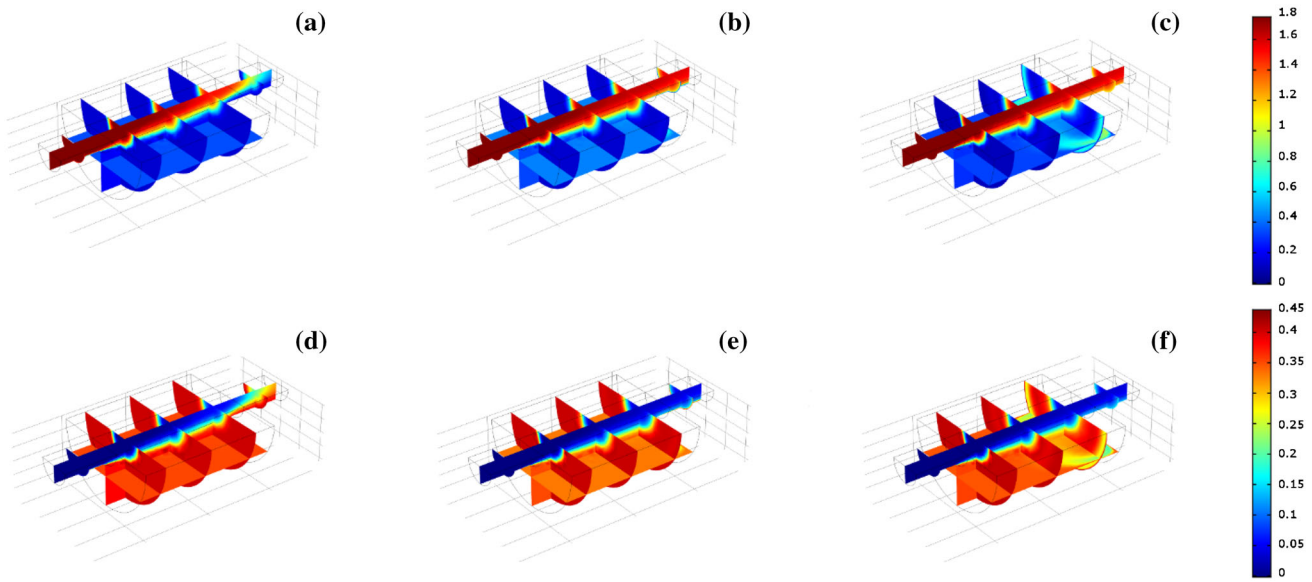

Fig. 4 Transient CO_2 concentration (mol/m^3) propagation in a reservoir with the volume v $= 0.5 \times 10^{-3}$ m^3 at three time instances: t = 0.5 s (**a**, **d**), t = 1.0 s (**b**, **e**), t = 2.4 s (**c**, **f**). **a**–**c** and **d**–**f** denote the exhale and inhale processes, respectively. The inflow boundary condition is assumed at the *left* side of the reservoir. In **a**–**c** the *left side* denotes the *inlet* of accordion-like device, and in **d**–**f**, left side denotes the outlet of accordion-like device presented in Fig. 1

ambient air, the CO_2 concentration in each breathing cycle can be obtained in a procedure explained below.

The average O_2 concentration in the chamber after an inhalation, $x_{O_2,2}$, is obtained from its value before inhalation $x_{O_2,1}$ as

$$x_{O_2,2} = \left[(\gamma TV)x_{O_2,in} + (RV - \gamma TV)x_{O_2,1}\right]/RV, \quad (8)$$

where $x_{O_2,in}$ is the inlet air O_2 concentration, which is equal to 8.83 mol/m^3 in standard air condition. Equation (8) relies on the flow incompressibility which implies that the

inflow and outflow volumes are both equal to TV. Due to an imperfect mixing of the inlet with the reservoir air, part of the inlet air, $(1-\gamma)TV$, leaves the reservoir without mixing with the reservoir air. Another part, γTV, flows towards outlet after mixing with the reservoir air. The coefficient γ can have a value in the range [0, 1], with $\gamma = 1$ denoting a perfect mix. The main reason to introduce γ in the equations is to (i) account for imperfect mixing in small volume, e.g. due to undeveloped flow; and (ii) account for any unforeseen parameter that can affect the mixing of the CO_2 and fresh air. Therefore, the average O_2 concentration, $y_{O_2,1}$, experienced during inhalation can be obtained as

$$y_{O_2,1} = 0.5\gamma\left(x_{O_2,1} + x_{O_2,2}\right) + (1-\gamma)x_{O_2,in} \tag{9}$$

Similar procedure is followed during exhalation. The exhale O_2 concentration, $y_{O_2,2}$, where

$$y_{O_2,2} = y_{O_2,1}\left(1 - \frac{5}{21}\right), \tag{10}$$

is mixed "imperfectly"' with the chamber in a similar fashion

$$x_{O_2,3} = \left[(\gamma TV)y_{O_2,2} + (RV - \gamma TV)x_{O_2,2}\right]/RV, \tag{11}$$

where $x_{O_2,3}$ is the O_2 concentration at the end of a breathing cycle. The O_2 reduction value in rebreathing was assumed to be 5/21, which is for a healthy subject. This value may change slightly between patients. The breathing procedure formulated by Eqs. (8)–(11) is then repeated, given the initial $x_{O_2,1}$ concentration at the beginning of the breathing is the one obtained at the end of the previous cycle, i.e. $x_{O_2,3}$. We assume that the flow rate during the inhalation and exhalation are similar; therefore, parameter γ has the same value in Eqs. (8), (9), and (11).

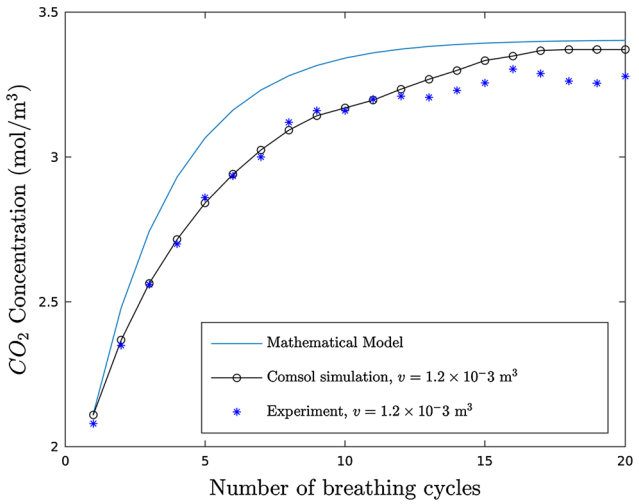

Fig. 5 Transient CO_2 accumulation in an apnea treatment device with the volume of v $= 1.2 \times 10^{-3}$ m^3. The plot shows the results of the mathematical model, simulation, and experiment

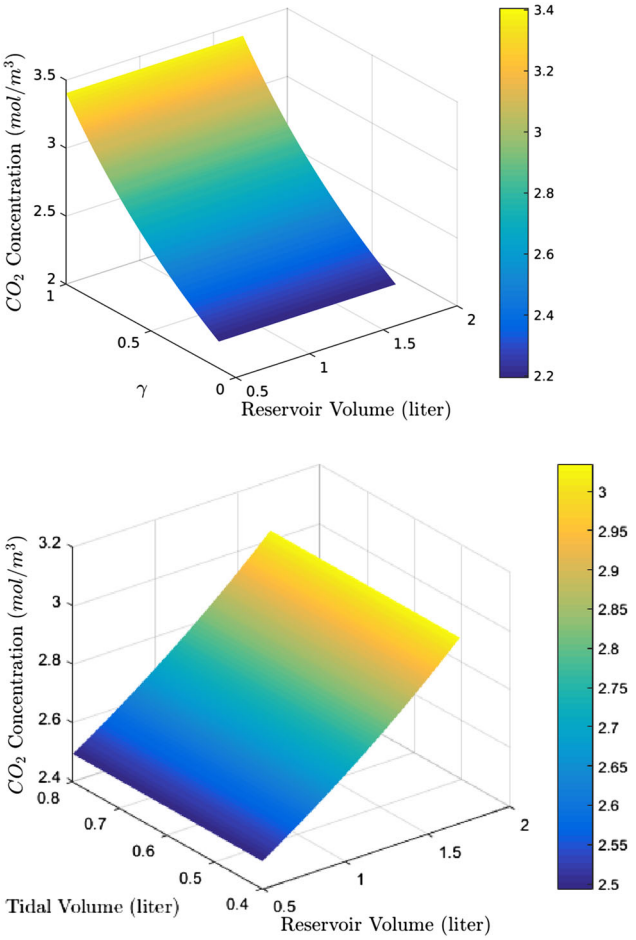

Fig. 6 Parametric analysis of the CO_2 accumulation in the apnea treatment device for different values of DS volume, RV, tidal volume, TV, and mixing efficiency, γ. The CO_2 accumulation is provided for: *top* $RV \in [0.5, 1.7]$ L and $\gamma \in [0, 1]$, and *bottom* $RV \in [0.5, 1.7]$ L and $TV \in [0.5, 1.7]$ L

Figure 5 shows the CO_2 accumulation in a device with RV $= 1200$ mL, where it is assumed that the mixing of the inflow and reservoir air is complete ($\gamma = 1$). A good agreement with the experimental data was obtained for the small device when $\gamma = 0.5$. We conjecture that the imperfect mixing of the CO_2 and fresh air in the small device due to undeveloped flow causes imperfect mixture and calls for $\gamma < 1$. This is shown in Fig. 4 where the bulk of the flow is around pipe center line.

The mathematical model and experimental results demonstrate the CO_2 buildup in the proposed device. We use this model to investigate the change of the CO_2 buildup when the environment condition changes to ensure that an excessive CO_2 concentration will never happen. To this end, we conducted a series of tests in the design domain defined by $\gamma \in [0, 1]$, $TV \in [0.3, 0.8] \times 10^{-3}$ and $RV \in [0.5, 1.7] \times 10^{-3}$ m^3. We found no situation where the CO_2 concentration exceeds 3.5 mol/m^3, see Fig. 6.

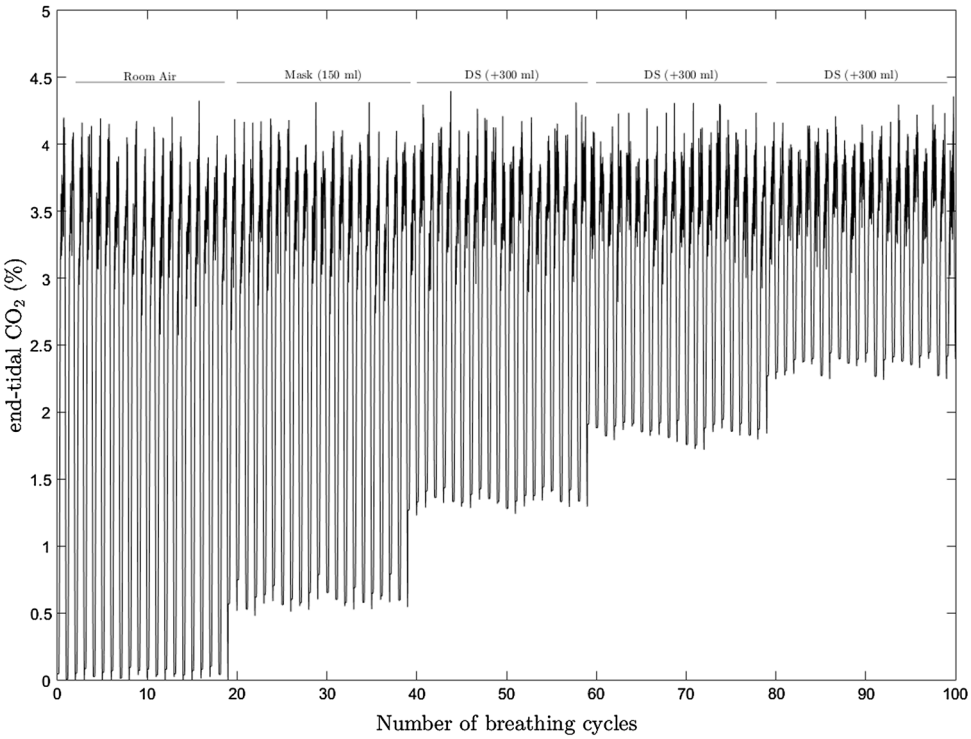

Fig. 7 HPS mannequin end-tidal carbon dioxide capnography. The plot shows a segment of room air breathing followed by a segment of breathing through a face mask with 150 mL DS, and then an additional 300 mL DS were added to the mask and the end-tidal CO_2 was recorded. This action was repeated for total of three times. The segment with added DS shows an elevation in $P_{ET}CO_2$

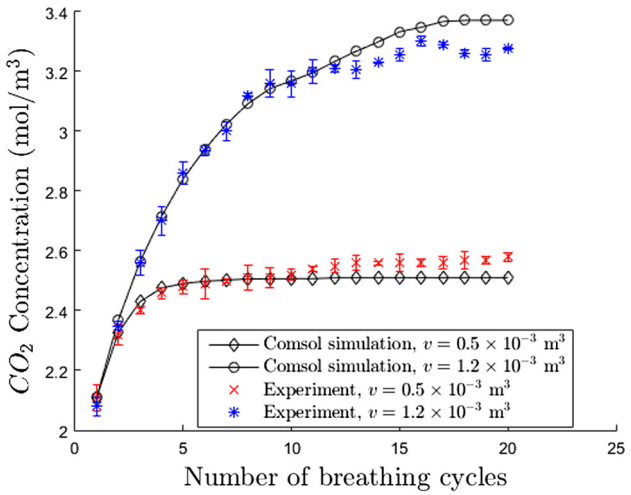

Fig. 8 Comparison of the average CO_2 accumulation obtained from COMSOL simulation and experimental data inside the apnea treatment device. CO_2 increased at the lower and higher volume level of added DS. At each level after adequate number of breathing cycle CO_2 level reach plateaued

The mathematical model provided to capture the CO_2 accumulation relies on the perfect mixing of the exhale air with the DS air. This condition is satisfied when the DS volume is large enough and the flow reaches a fully developed condition. However, when the DS volume is small, a great portion of the inlet air passes through the device without mixing with the existing air, see Fig. 4. To account for this, we assumed that the mixing coefficient for small volumes changes linearly with the DS volume until it reaches its maximum at 1.2×10^{-3} m^3.

To summarize, a variable volume DS reservoir device was designed, constructed and tested. The result of this test was achieved through exposing the mannequin to inhaled gas from a CO_2 reservoir; a process that increased end-tidal CO_2 ($P_{ET}CO_2$) during normal breathing Fig. 7. Based on previous studies [2], this adjustable variable volume device may permit the use of minimal amount of dead space (and therefore minimal increase in CO_2 to eliminate significant numbers of apneas, thereby providing an opportunity for apnea elimination without side effects of "excessive" hypercapnia as described in Khayat et al. study [22].

The experimental and simulation values of the CO_2 concentration for two device designs with minimum and maximum DS volume, $v = [0.5,\ 1.2] \times 10^{-3}$ m^3, are captured in Fig. 8. For both device volumes, the concentration values measured experimentally and computationally agree well. Additionally, confirmed by those tests, the CO_2 concentration can be adjusted by changing the DS volume.

4 Discussion

Dead space device has been used in several studies since 1980s which incorporates the rebreathing of exhaled air to induce moderate hypercapnic conditions in systemic circulation [2, 8] have recently demonstrated in a small cohort

of OSA patients that breathing from a CO_2-enriched reservoir eliminates most apneic events in obstructive and central sleep apnea patients [8]. However, none of those aforementioned studies provide a model to study the behavior of CO_2 inside the DS device. To back up the experimental studies conducted on the breathing mannequin, the rebreathing process was numerically simulated. The simulation tool can provide a priori knowledge of the CO_2 accumulation for the rebreathing DS device. Furthermore, a mathematical model was provided to analyze, more efficiently, the CO_2 accumulation. The model was used to run three parametric studies (*RV, TV,* and γ) to ensure that excessive CO_2 accumulation is avoided. Suggested mathematical models can assess the CO_2 rebreathing device function for further study.

The merit of numerical modeling approach is to quantify the mixing pattern of the CO_2 in the device and analyze the CO_2 accumulation, through a wide range of input parameters and patient data. This study was conducted to evaluate and provide a better understanding of the transient CO_2 propagation and the mixing of the inflow and reservoir air. A series of validation scenarios using a combination of experiment and simulation were conducted for different DS volumes. We conjecture that a similar simulation technique may be used to study the problems that involve human exhale air in different apparatus.

The limitation of the study is that we did not collect qualitative or quantitative data on human subject, subject comfort, or subject breathing effort using the device. Furthermore, for each device design study, the geometry needs to be built in the software, and appropriate mesh selected. The re-meshing of the reservoir may ask for a long processing time. More refine mesh increases the computation time exponentially since it also demands for small time step.

5 Conclusions

We designed, fabricated, and tested a relatively inexpensive, inspired CO_2 rebreathing device for the purpose of sleep apnea treatment. We performed a CFD analysis and an experimental test bench. This study was conducted to evaluate how volumetric differences in the DS device, used for sleep apnea treatment, affects the dynamics of CO_2 accumulation in the device by means of mathematical/simulation/computational modeling and experimental approaches. We have tested the accuracy of this device by providing a model to study the behavior of CO_2 inside the DS device. A breathing mannequin, with mechanics similar to patients, was used to simulate respiration for testing. The mannequins quantified, via mathematical modelling, the dynamics of CO_2 mixing between the inflow gas and dead space air. The main advantage of this proposed variable DS device is to elicit highly predictable ($\pm$ 3.5% error) alveolar P_aCO_2 levels by changing the reservoir DS, thereby ensuring that excessive CO_2 accumulation would not occur during rebreathing. The use of suggested mathematical models can assess the CO_2 rebreathing device function for further study in the respiratory system and devices.

Acknowledgements This work has been partially supported by the Center of Energy and Sustainability at California State University—Los Angeles, through an NSF HRD-1547723 Grant.

Appendix

This section further demonstrates and explains the details and mesh type associated to the implementation of the finite element method. Table 1 includes details about the mesh used in the computational study, such as type of elements, number of elements, mesh quality metrics, etc. (Fig. 9).

Table 1 Mesh statistics' details about the mesh used in the computational study [28]

Description	Value
Minimum element quality	0.02965
Average element quality	0.5922
Tetrahedral elements	30,302
Pyramid elements	186
Prism elements	7562
Triangular elements	6136
Quadrilateral elements	352
Edge elements	487
Vertex elements	18
Maximum element size	0.00608
Minimum element size	0.00182
Maximum element growth rate	1.2

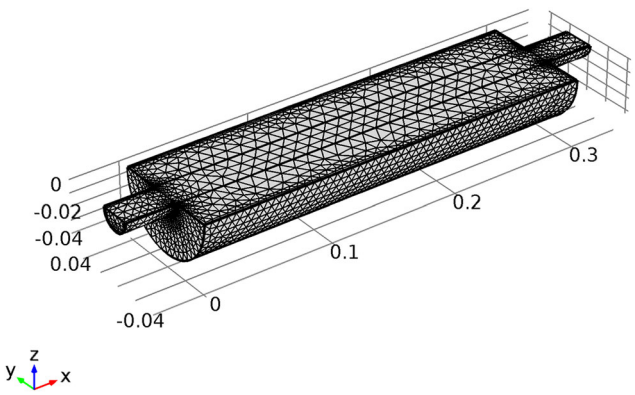

Fig. 9 Demonstrates the mesh used in the computational study

References

1. Peppard, P. E., Young, T., Barnet, J. H., Palta, M., Hagen, E. W., & Hla, K. M. (2013). Increased prevalence of sleep-disordered breathing in adults. *American Journal of Epidemiology, 177*(9), 1006–1014.
2. Mulchrone, A., Shokoueinejad, M., & Webster, J. (2016). A review of preventing central sleep apnea by inspired CO_2. *Physiological Measurement, 37*(5), R36.
3. Berssenbrugge, A., Dempsey, J., Iber, C., Skatrud, J., & Wilson, P. (1983). Mechanisms of hypoxia-induced periodic breathing during sleep in humans. *The Journal of Physiology, 343,* 507.
4. Badr, M. S., Grossman, J. E., & Weber, S. A. (1994). Treatment of refractory sleep apnea with supplemental carbon dioxide. *American Journal of Respiratory and Critical Care Medicine, 150*(2), 561–564.
5. Lorenzi-Filho, G., Rankin, F., Bies, I., & Bradley, T. D. (1999). Effects of inhaled carbon dioxide and oxygen on Cheyne–Stokes respiration in patients with heart failure. *American Journal of Respiratory and Critical Care Medicine, 159*(5), 1490–1498.
6. Steens, R. D., Millar, T. W., Su, X., Biberdorf, D., Buckle, P., Ahmed, M., et al. (1994). Effect of inhaled 3% CO_2 on Cheyne-Stokes respiration in congestive heart failure. *Sleep, 17*(1), 61–68.
7. Xie, A., Rankin, F., Rutherford, R., & Bradley, T. D. (1997). Effects of inhaled CO2 and added dead space on idiopathic central sleep apnea. *Journal of Applied Physiology, 82*(3), 918–926.
8. Xie, A., Teodorescu, M., Pegelow, D. F., Teodorescu, M. C., Gong, Y., Fedie, J. E., et al. (2013). Effects of stabilizing or increasing respiratory motor outputs on obstructive sleep apnea. *Journal of Applied Physiology, 115*(1), 22–33.
9. Eckert, D. J., White, D. P., Jordan, A. S., Malhotra, A., & Wellman, A. (2013). Defining phenotypic causes of obstructive sleep apnea. Identification of novel therapeutic targets. *American Journal of Respiratory and Critical Care Medicine, 188*(8), 996–1004. doi:10.1164/rccm.201303-0448OC.
10. Dempsey, J. A., Xie, A., Patz, D. S., & Wang, D. (2014). Physiology in medicine: Obstructive sleep apnea pathogenesis and treatment–considerations beyond airway anatomy. *Journal of Applied Physiology (1985), 116*(1), 3–12. doi:10.1152/japplphysiol.01054.2013.
11. Skatrud, J. B., & Dempsey, J. A. (1983). Interaction of sleep state and chemical stimuli in sustaining rhythmic ventilation. *Journal of Applied Physiology: Respiratory, Environmental and Exercise Physiology, 55*(3), 813–822.
12. Iber, C., Davies, S. F., Chapman, R. C., & Mahowald, M. M. (1986). A possible mechanism for mixed apnea in obstructive sleep apnea. *Chest, 89*(6), 800–805.
13. Berssenbrugge, A., Dempsey, J., Iber, C., Skatrud, J., & Wilson, P. (1983). Mechanisms of hypoxia-induced periodic breathing during sleep in humans. *Journal of Physiology, 343,* 507–524.
14. Sankari, A., Bascom, A. T., Chowdhuri, S., & Badr, M. S. (2014). Tetraplegia is a risk factor for central sleep apnea. *Journal of Applied Physiology (1985), 116*(3), 345–353. doi:10.1152/japplphysiol.00731.2013.
15. Khayat, R. N., Xie, A., Patel, A. K., Kaminski, A., & Skatrud, J. B. (2003). Cardiorespiratory effects of added dead space in patients with heart failure and central sleep apnea. *Chest, 123*(5), 1551–1560.
16. Xie, A., Rankin, F., Rutherford, R., & Bradley, T. D. (1997). Effects of inhaled CO2 and added dead space on idiopathic central sleep apnea. *Journal of Applied Physiology (1985), 82*(3), 918–926.
17. Lorenzi-Filho, G., Rankin, F., Bies, I., & Douglas Bradley, T. (1999). Effects of inhaled carbon dioxide and oxygen on cheyne-stokes respiration in patients with heart failure. *American Journal of Respiratory and Critical Care Medicine, 159*(5 Pt 1), 1490–1498. doi:10.1164/ajrccm.159.5.9810040.
18. Haxhiu, M. A., van Lunteren, E., Mitra, J., & Cherniack, N. S. (1987). Comparison of the response of diaphragm and upper airway dilating muscle activity in sleeping cats. *Respiration Physiology, 70*(2), 183–193.
19. Horner, R. L., Liu, X., Gill, H., Nolan, P., Liu, H., & Sood, S. (2002). Effects of sleep-wake state on the genioglossus vs.diaphragm muscle response to CO(2) in rats. *Journal of Applied Physiology (1985), 92*(2), 878–887. doi:10.1152/japplphysiol.00855.2001.
20. Szollosi, I., Jones, M., Morrell, M., Helfet, K., Coats, A., & Simonds, A. (2004). Effect of CO2 inhalation on central sleep apnea and arousals from sleep. *Respiration, 71*(5), 493–498.
21. Andreas, S., Weidel, K., Hagenah, G., & Heindl, S. (1998). Treatment of Cheyne-Stokes respiration with nasal oxygen and carbon dioxide. *European Respiratory Journal, 12*(2), 414–419.
22. Khayat, R. N., Xie, A., Patel, A. K., Kaminski, A., & Skatrud, J. B. (2003). Cardiorespiratory effects of added dead space in patients with heart failure and central sleep apnea. *CHEST Journal, 123*(5), 1551–1560.
23. Xie, A., Skatrud, J. B., & Dempsey, J. A. (2001). Effect of hypoxia on the hypopnoeic and apnoeic threshold for CO_2 in sleeping humans. *The Journal of Physiology, 535*(1), 269–278.
24. Skadberg, B., Oterhals, Å., Finborud, K., & Markestad, T. (1995). CO2 rebreathing: A possible contributory factor to some cases of sudden infant death? *Acta Paediatrica, 84*(9), 988–995.
25. Webster, J., dos Santos, I., Shokoueinejad, M., Levin, J., Dempsey, J., Wang, F., et al. (2016). Sleep apnea therapy device that automatically adjusts the fraction of inspired carbon dioxide. US Patent 15/376,180.
26. Stocker, T. (2011). *Introduction to climate modelling*. New York: Springer.
27. Marrero, T. R., & Mason, E. A. (1972). Gaseous diffusion coefficients. *Journal of Physical and Chemical Reference Data, 1*(1), 3–118.
28. Comsol. (2011). *COMSOL multiphysics: Version 4.2*. Burlington, MA: Comsol.
29. Nunn, A., & Gregg, I. (1989). New regression equations for predicting peak expiratory flow in adults. *BMJ, 298*(6680), 1068–1070.